Tlebaldiyeva, Leila; Maham, Behrouz; Tirkkonen, Olav

Maximum Sub-array Diversity for mmWave Network under RF Power Leakage and Transceiver Distortion Noises

Published in:
2020 IEEE Wireless Communications and Networking Conference, WCNC 2020 - Proceedings

DOI:
10.1109/WCNC45663.2020.9120487

Published: 01/05/2020

Document Version
Peer-reviewed accepted author manuscript, also known as Final accepted manuscript or Post-print

Maximum Sub-array Diversity for mmWave Network under RF Power Leakage and Transceiver Distortion Noises

Leila Tlebaldiyeva*, Behrouz Maham*, and Olav Tirkkonen†
*Department of Electrical and Computer Engineering, Nazarbayev University, Nur-Sultan, Kazakhstan
†Department of Communications and Networking, Aalto University, Aalto, Finland
Email: ltlebaldiyeva@nu.edu.kz, behrouz.maham@nu.edu.kz, olav.tirkkonen@aalto.fi

***Abstract*—This paper investigates RF power leakage in millimeter wave (mmWave) networks operating on hybrid beamforming (HB) system where a base station with massive MIMO antennas communicates with user equipment (UE) nodes equipped with a single antenna. RF power leaks between spatially divided transmissions to different users, due to back/side lobes of antennas. A maximum sub-array transmission diversity technique implemented on HB is proposed to improve the system performance under RF power leakage and residual transceiver distortion noise. In this work, we emphasize how RF power leakage and residual transceiver distortion noise constraints degrade the quality of communication performance in terms of outage probability (OP) and ergodic capacity. An analytic model of mmWave connectivity is used, resulting in closed-form expressions for the OP and ergodic capacity. These are corroborated through Monte-Carlo simulations. Simulation results demonstrate that the effect of transceiver distortion noise is more severe at high signal power due to the proportionality of transceiver distortion noise to signal power.**

***Index Terms*—Diversity, hybrid beamforming, millimeter wave communication, Nakagami-m fading channel.**

I. INTRODUCTION

Millimeter wave (mmWave) frequencies and massive multiple-input-multiple-output (MIMO) antennas are driving technologies for future networks. Commercial 5G networks are already being deployed by some operators in South Korea, the USA, and the UK. Beamforming and beam steering are major techniques while implementing mmWave networks. Three major types of beamforming structures: digital [1], analog [2], and hybrid beamforming (HB) [3] are considered in the literature to implement beamforming/steering in the mmWave domain. Theoretically, digital beamforming allows precise beamforming, thus the best performance, at the cost of a high number of RF chains that accumulate an additional cost for a network implementation. On the other hand, analog beamforming is cheaper to implement; however, calibration of phase shifters is time-consuming and imprecise. Therefore, HB is an optimal solution to combine the advantages of both digital/analog beamforming structures and it has gained considerable attention in the literature. HB offers a higher degree of freedom due to multistream digital processing, as well as analog processing of a large number of antenna elements which provides array gain by using analog phase shifters. Moreover, HB allows the implementation of multi-user communication within the cell. MmWave frequencies suffer from high propagation loss caused by water vapor and oxygen absorption. In addition, signal blockage (e.g., self-blockage, static blockage, and dynamic blockage) complicates mmWave communication. Therefore, it is essential to implement independent diversity paths between a transmitter and receiver in mmWave communication to guarantee a quality of service. The authors in [4] proposed dual-function HB and transmit diversity network architecture, where the antenna array is divided into sub-arrays that are farther located from each other to experience independent fading. The authors in [5] presented a novel hybridly connected structure for mmWave massive MIMO. The spectral efficiency of the hybridly connected structure outperforms the partially connected one. Ideal transceiver hardware is assumed in the aforementioned works and most of the technical literature; however, practical transceivers experience non-linearity in power amplifiers, phase noise, in-phase and quadrature (I/Q) imbalance, and ADC/DAC quantization errors. According to [6], mmWave frequencies are more susceptible to transceiver distortion noise than centimeter wave frequencies. The aggregate residual hardware impairments in mmWave massive MIMO systems have been modelled as additive white Gaussian noise proportional to average signal power [7]. Moreover, RF power leakage is has to be taken into account when considering multi-user communication. RF power leakage occurs when an analog beamformed signal emitted to a neighboring user equipment (UE) is combined with the desired UE signal. The literature on RF power leakage of neighboring nodes given HB for multi-user communication is limited. A leakage-based precoding scheme for multi-user mmWave channels was investigated in [8] for an ideal system model.

In this work, we shall investigate downlink communication among a mmWave base station and UE terminals by utilizing HB diversity techniques. In addition, the proposed mmWave network is constrained by transceiver distortion noise originating from transceiver hardware as well as RF power leakage.

We make the following assumption for the mmWave channel: after the analog precoding part of HB is done, the channel model seen from the digital precoder part is statistically

The work of Olav Tirkkonen was funded in part by the Academy of Finland (grant 319484).

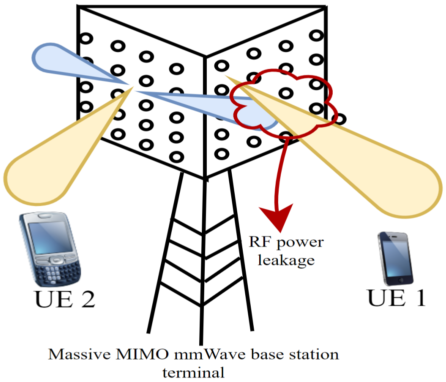

Fig. 1. Hybrid beamforming mmWave network model under RF power leakage constraint by using SDMA to separate users.

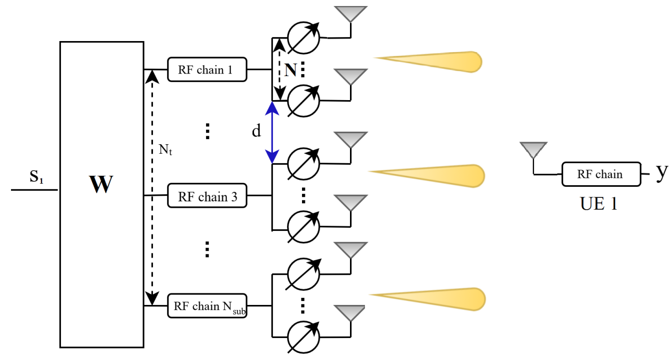

Fig. 2. Hybrid beamforming network with maximum sub-array transmission diversity technique directed to UE 1.

modelled as a fading channel scaled by the antenna array gain from the analog beamforming network. Inspired by recent studies in [9]–[12] a Nakagami-m fading channel model is used to describe the mmWave channel. The advantage of Nakagami-m fading channel is not only its analytical tractability but also the ability to model line-of-sight (LOS)/non-LOS (NLOS) components of the mmWave channel. According to outdoor experiment results taken place at the 5G trial area in Tokyo Odaiba at 28 GHz frequency in [13], both NLOS and LOS are crucial factors influencing mmWave communication performance. The main contributions of this work are outlined as follows:

- We introduce a multi-user mmWave network model based on the HB that accounts for RF power leakage from neighboring UEs and aggregate transceiver distortion noise.
- The proposed maximum sub-array transmission (MST) diversity technique enables to combine multiple and independent sub-arrays to enhance the reliability measured by outage probability. The MST diversity technique combats both the path loss and RF power leakage.
- After formulating the instantaneous signal-to-power leakage-distortion and noise-ratio (SPDNR) for HB mmWave network and deriving its distribution, we evaluate the outage probability (OP) and ergodic capacity with its lower bound. We verify analytical closed-form expressions through Monte-Carlo simulations.

II. System Model

We consider a multi-user mmWave network for downlink transmission from a base station to a UE as shown in Fig. 1. The base station uses space division multiple access (SDMA) for simultaneous communication with UEs. For simplicity, we consider two UEs in the system; UE 1 is the desired user, and simultaneous transmission to UE 2 causes RF power leakage to UE 1 as depicted in Fig. 1.

In Fig. 2, we present a HB structure between the base station and the UE 1. The base station dedicates N_t antennas for each UE to implement MST diversity with the order of $N_s = N_t/N$, where N is the number of antennas per sub-array. Thus, multiple antennas are used to make a series of analog beamformers with the same alignment toward the desired user, by dividing them into N_s sub-arrays.

Similar to [4], we assume that two consecutive sub-arrays are separated by several wavelengths, e.g., $d > 5\lambda$, where λ stands for wavelength and d denotes the distance between sub-arrays such that each RF chain experiences an independent and uncorrelated path. This is a feasible assumption since, in mmWave bands, wavelengths correspond to very small distances. The sub-array division of the analog beamformer network enables us to establish independent and uncorrelated Nakagami-m distributed diversity channels between the base station and UE. Next, we assume a sectored pattern model similar to [14] for modelling the array pattern of each analog beamforming sub-array:

$$G(\theta) = \begin{cases} G_m, & |\theta| \leq \theta_b, \\ G_s, & \text{otherwise}, \end{cases} \tag{1}$$

where θ is a boresight angle, θ_b is an antenna beamwidth, G_m is a main lobe antenna gain and G_s is a side/back lobe antenna gain. Thus, the antenna gain is modelled by constant values in the main lobe and side/back lobe sector. Besides, we assume perfect beam sweeping process for the base station and UEs to estimate the angle of arrival. The base station uses control channels to align a desired user to the main lobe sector. Each sub-array contains N antennas connected to a phase shifter network that forms a beam towards the desired UE. At the receiver side, we consider a single antenna user connected to the RF chain. In Fig. 2, the data stream s_1 with the average signal power P_1 feeds into a linear digital precoder $\boldsymbol{w}$ with the size $N_s \times 1$. The digital precoder weight for sub-array k is defined as

$$w_k = \frac{h_k^*}{\|h_k\|}, \tag{2}$$

where h_k is modelled as a Nakagami-m distributed channel amplitude with integer shape parameter $m_k \geq 1$ and arbitrary scale parameter $\beta_k > 0$. The Euclidian norm is denoted by $\|\cdot\|$. Similar to [9], we consider fixed LOS and NLOS fading channel coefficients as $m \in \{m_L, m_N\}$, where m_L stands for LOS and m_N denotes NLOS fading parameters. In addition, we set the path loss exponent, α_0, as LOS and NLOS given as $\alpha_0 \in \{\alpha_L, \alpha_N\}$, respectively. Next, the digitally precoded signal is multiplied by an analog precoder vector with antenna gain G_m assuming that the main lobe beam is aligned to the desired UE. After a digitally precoded signal is fed to N_s phase shifter networks, N_s independent beams are received at the UE 1. Thus, we formulate the received signal for the non-ideal system model under RF power leakage and aggregate transceiver distortion noise as follows

$$y = \sqrt{Q}\boldsymbol{h}^t\left(\boldsymbol{w}\sqrt{G_m}(s_1+\epsilon_1)+\boldsymbol{w}'\sqrt{G_s}(s_2+\epsilon_2)\right)+n, \tag{3}$$

where $\boldsymbol{h} = [h_1, h_2, \cdots, h_{N_s}]$ is a $N_s \times 1$ vector and $(\cdot)^t$ denotes the transpose operator, $\boldsymbol{w}$ is a $N_s \times 1$ vector, and n is the additive white Gaussian noise with the zero mean and σ^2 variance. In addition, we denote UE 2 channel coefficient vector with the size $N_s \times 1$ as $\boldsymbol{g} = [g_1, g_2, \cdots, g_{N_s}]$ which stands for Nakagami-m fading channel coefficients between a base station and a UE 2. We apply $\boldsymbol{g}$ to evaluate the digital precoder vector for UE 2 as $\boldsymbol{w}' = \frac{\boldsymbol{g}^*}{\|\boldsymbol{g}\|}$. Moreover, s_2 is the UE 2 signal with average signal power, P_2. The path loss is evaluated as $Q = L^{-\alpha_0}$, where L is a communication distance, α_0 is a path loss exponent, and G_s is a side/back lobe antenna gain. Furthermore, aggregate transceiver distortion noises are modelled as $\epsilon_{1,2} \sim \mathcal{CN}(0, \kappa^2 P_{1,2})$, where κ is a measure of error vector magnitude (EVM)[1]. Now, by using (2), we get the following expression for the received signal

$$y = \sqrt{Q}\|\boldsymbol{h}\|\sqrt{G_m}(s_1+\epsilon_1)+\sqrt{Q}\frac{\boldsymbol{g}^*}{\|\boldsymbol{g}\|}\boldsymbol{h}^t\sqrt{G_s}(s_2+\epsilon_2)+n. \tag{4}$$

From (4), the SPDNR can be calculated as,

$$\gamma^{\mathrm{RD}} = \frac{P_1 Q G_m \sum_{k=1}^{N_s}|h_k|^2}{P_1 Q\kappa^2 G_m\sum_{k=1}^{N_s}|h_k|^2 + \frac{P_2 Q G_s|\sum_{k=1}^{N_s} h_k g_k^*|^2(1+\kappa^2)}{\sum_{k=1}^{N_s}|g_k|^2} + \sigma^2}. \tag{5}$$

By using the Cauchy-Schwarz inequality, $|\sum_{k=1}^{N_s} h_k g_k^*|^2 \leq \sum_{k=1}^{N_s}|h_k|^2\sum_{k=1}^{N_s}|g_k^*|^2$, the SPDNR can be simplified to

$$\gamma^{\mathrm{RD}} \geq \frac{a\sum_{k=1}^{N_s}X_k}{b\sum_{k=1}^{N}X_k + c\sum_{k=1}^{N}X_k + 1}, \tag{6}$$

where for notational simplicity, we denote $a = \frac{P_1 G_m Q}{\sigma^2}$, $b = \frac{\kappa^2 P_1 G_m Q}{\sigma^2}$, $c = \frac{P_2 G_s Q(1+\kappa^2)}{\sigma^2}$, and $X_k = |h_k|^2$. The channel power gain for Nakagami-m distribution is a Gamma distributed random variable (RV) X_k. We consider independent and identically distributed (i.i.d.) fading channel power gains X_k, for $k = 1, \cdots, N_s$. The cumulative distribution function (CDF) and probability density function (PDF) of the sum of N i.i.d. X_k RVs are presented in Lemma 1 below.

Lemma 1. *Let us consider a finite set of N_s non-negative i.i.d. Gamma RVs $\{X_k\}_{k=1}^{N_s}$. The sum of these RVs $Y = \sum_{k=1}^{N_s} X_k$ is another Gamma distributed RV with CDF*

$$F_Y(y) = \frac{1}{\Gamma(mN_s)}\gamma\left(mN_s, \frac{y}{\beta}\right), \tag{7}$$

where $m = m_k$, $\beta = \beta_k$, $\Gamma(\cdot)$ is the Gamma function and $\Gamma(\cdot,\cdot)$ is the incomplete Gamma function. Moreover, the PDF for RV Y is

$$f_Y(y) = \frac{1}{\Gamma(mN_s)\beta^m}y^{mN_s-1}e^{-\frac{y}{\beta}}. \tag{8}$$

III. Outage Probability Performance

In this section, we evaluate the closed-form expression for the OP given a system with RF-power leakage and transceiver distortion noise constraints. The OP for the proposed system is evaluated as $P_{out} = \Pr(\gamma^{\mathrm{RD}} \leq \gamma_{th})$, where γ_{th} is a predefined threshold on γ^{RD}.

Proposition 1. *Consider a finite set of i.i.d. Gamma distributed RVs $X_k = \{X_1, \cdots X_{N_s}\}$ as well positive and real constants a, b, and c. The CDF of*

$$\gamma^{\mathrm{RD}} = \frac{a\sum_{k=1}^{N_s}X_k}{b\sum_{k=1}^{N_s}X_k + c\sum_{k=1}^{N_s}X_k + 1} \tag{9}$$

yields the OP that could be calculated as

$$\Pr(\gamma^{\mathrm{RD}} < \gamma_{th}) = \begin{cases} \frac{\gamma\left(mN_s, \frac{\gamma_{th}}{(a-b\gamma_{th}-c\gamma_{th})\beta}\right)}{\Gamma(mN_s)}, \gamma_{th} < \frac{a}{b+c} \\ 1, \quad \gamma_{th} > \frac{a}{b+c}. \end{cases} \tag{10}$$

Proof. Let us denote Y as the summation of N_s i.i.d. Gamma RVs X_k. With the aid of Lemma 1, we define the CDF of Y as $Y \sim Gamma(mN_s, \beta)$, where m is the shape parameter, N_s is the integer value, and β is the scale parameter. The CDF of γ^{RD} is

$$\begin{aligned}\Pr(\gamma^{\mathrm{RD}} < \gamma_{th}) &= \Pr\left(\frac{aY}{bY+cY+1} < \gamma_{th}\right) \\ &= \begin{cases} \Pr\left(Y < \frac{\gamma_{th}}{a-b\gamma_{th}-c\gamma_{th}}\right), \quad \gamma_{th} < \frac{a}{b+c} \\ 1, \quad \gamma_{th} \geq \frac{a}{b+c}. \end{cases}\end{aligned} \tag{11}$$

□

IV. Ergodic Capacity Analysis

In this section, we calculate the generic ergodic capacity and it's lower bound for the MST diversity mmWave network under presence of aggregate transceiver distortion noise and RF power leakage. By definition, the ergodic capacity is evaluated as $C = \mathbb{E}\{\log_2(1+\gamma^{\mathrm{RD}})\}$, where $\mathbb{E}\{\cdot\}$ stands for the expectation operator. Using (6), ergodic capacity is calculated as

$$\begin{aligned}C &= \mathbb{E}\left\{\log_2(1+\frac{aY}{(b+c)Y+1}\right\} \\ &= \mathbb{E}\left\{\log_2((a+b+c)Y+1) - \log_2((b+c)Y+1)\right\}.\end{aligned} \tag{12}$$

Proposition 2. *Let us consider a multi-user mmWave network constrained by RF power leakage and transceiver distortion*

[1] EVM is a measure of the hardware impairment noises originated from IQ phase shift, amplifier non-linearity, AWGN, and phase noise [15]. EVM is a Figure of Merit that evaluates transceiver performance measured in dB or percentage.

TABLE I
SYSTEM PARAMETERS OF THE PROPOSED SYSTEM MODEL

Parameter	Value	Description
α_L	2	LOS path-loss exponent
α_N	4	NLOS path-loss exponent
L	50 m	Distance
m_L	4	LOS fading parameter
m_N	2	NLOS fading parameter
W	100 MHz	Bandwidth
f	28 GHz	Operating frequency
G_m	16 dB	Main lobe gain
G_s	-5 dB	Side lobe gain
N_s	2	Number of sub-arrays
γ_{th}	6 dB	Threshold

noise. The SPDNR for this system model is expressed in terms of positive and real constants a,b,c and RV Y. The ergodic capacity is evaluated as

$$\begin{aligned} C=&\frac{1}{\Gamma(mN_s)}\sum_{i=0}^{mN_s-1}\frac{(mN_s-1)!}{(mN_s-1-i)!}\\ &\times\left(\frac{(-1)^{mN_s-i-2}e^{\frac{1}{(a+b+c)\beta}}}{((a+b+c)\beta)^{mN_s-1-i}}Ei\left(-\frac{1}{(a+b+c)\beta}\right)\right.\\ &+\sum_{k=1}^{mN_s-1-i}\frac{(k-1)!}{(-(a+b+c)\beta)^{mN_s-1-i-k}}\\ &-\frac{(-1)^{mN_s-i-2}e^{\frac{1}{(b+c)\beta}}}{((b+c)\beta)^{mN_s-1-i}}Ei\left(-\frac{1}{(b+c)\beta}\right)\\ &\left.-\sum_{k=1}^{mN_s-1-i}\frac{(k-1)!}{(-(b+c)\beta)^{mN_s-1-i-k}}\right), \end{aligned} \tag{13}$$

where $Ei(\cdot)$ is the exponential integral function defined in [16, Eq. 8.212.2].

Proof. The detailed derivation of the ergodic capacity C for the proposed system model is given in Appendix A. □

A. Lower Bound for Ergodic Capacity

By using the fact that $\log_2(1+a\exp(x))$, $a>0$, is a convex function for variable x and by applying the Jensen inequality, we present a general expression for the lower bound of ergodic capacity for non-ideal MST diversity mmWave system as

$$C_l=\log_2\left(1+\exp(\mathbb{E}\{\ln(aY)\}\right)-\mathbb{E}\{\ln\left((b+c)\,Y+1\right)\}. \tag{14}$$

Proposition 3. *A lower bound for the ergodic capacity under Nakagami-m fading channel for the proposed system model is evaluated as*

$$\begin{aligned} C_l^{\mathrm{Nak}}=&\log_2(1+\exp(\ln(a\beta)+\\ &\psi(mN_s))-\ln(1+(b+c)mN_s\beta)), \end{aligned} \tag{15}$$

where $\psi(\cdot)$ is Euler psi function given in [16, Eq. 8.360].

Proof. The proof is relegated in Appendix B. □

V. SIMULATION RESULTS

In this section, theoretical results from Sections III and IV are validated by Monte Carlo simulations. First, we consider the impact of aggregate transceiver distortion noise and RF power leakage level on the performance of the OP. The network parameters used in the simulation are presented in Table 1. We assume LOS links between the base station and UEs. Since UE 1 power level P_1 and β parameters are implicitly dependent on the received signal-to-noise ratio (SNR), we do not directly specify them. By definition, SNR $=\frac{P_1\mathbb{E}\{Y\}}{\sigma^2}$, where $\mathbb{E}\{Y\}=mN_s\beta$. In Fig. 3, we present the OP results for hardware impairment level $\kappa=0.1$ and $\kappa=0.3$; and for the level of RF power leakage from UE 2 being $P_2=10, 25$ dB. We notice that symmetric distortion level at different RF power leakage levels symmetrically degrade the OP performance. Based on this figure, both transceiver distortion noise and RF power leakage deteriorate the OP performance.

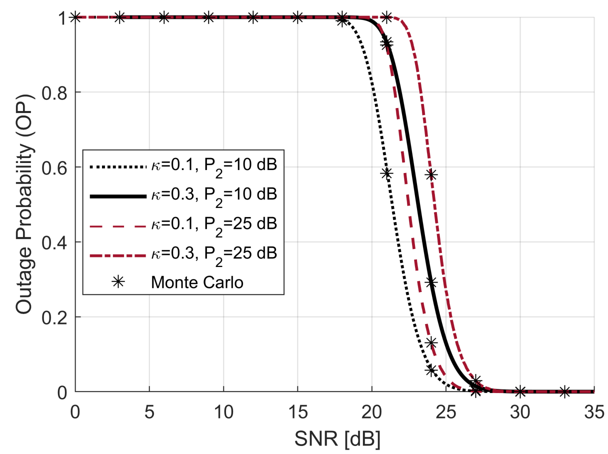

Fig. 3. Outage probability curves versus receive SNR for different levels of transceiver distortion noise and UE 2 average power.

In Fig. 4, we analyze how the number of diversity branches between a base station and a UE 1 affects the performance of the system. We set the UE 2 average power to $P_2=10$ dB and use network parameter values as given in Table 1, except we vary number of sub-arrays, N_s. In Fig. 4, we consider three plots with $N_s=1,2,4$ for $\kappa=0.1,0.3$. As shown in this figure, increasing the number sub-arrays enhances the OP performance. For instance, the plot with $N_s=4$ demonstrates the best OP performance.

In Fig. 5, we analyze the ergodic capacity versus SNR given $P_2=10, 20$ dB and $\kappa=0.01, 0.2, 0.3$. The negative impact of hardware impairment noise on ergodic capacity is clearly demonstrated in this figure. Moreover, a higher power of neighbouring UE 2 node causes more RF power leakage towards UE 1. When SNR $=20$ dB and $P_2=10$ dB, the ergodic capacity shows the following performance for different levels of hardware impairments: for $\kappa=0.3$ we get the ergodic capacity $C=3.55$ bits/sec/Hz, for $\kappa=0.2$ $C=4.59$ bits/sec/Hz, and for $\kappa=0.01$ $C=8.2$ bits/sec/Hz. Similarly, for SNR $=20$ dB and $P_2=20$ dB, we get the following ergodic capacity results: for $\kappa=0.3$ $C=3.20$ bits/sec/Hz, for $\kappa=0.2$ $C=3.9$ bits/sec/Hz, and for $\kappa=0.01$ $C=5.0$ bits/sec/Hz.

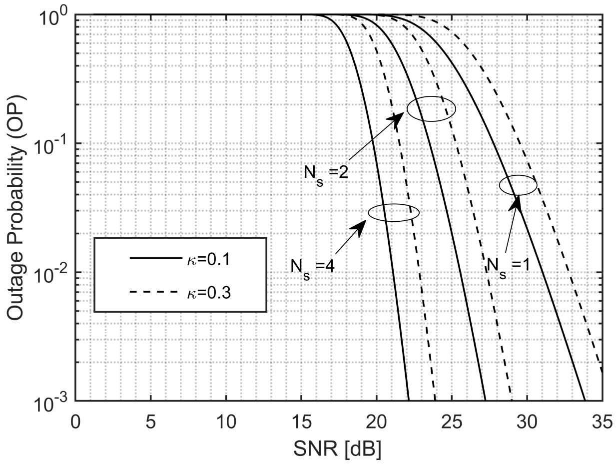

Fig. 4. Outage probability for a hybrid beamforming mmWave network model for $L = 50$ m and different levels of transceiver distortion noise.

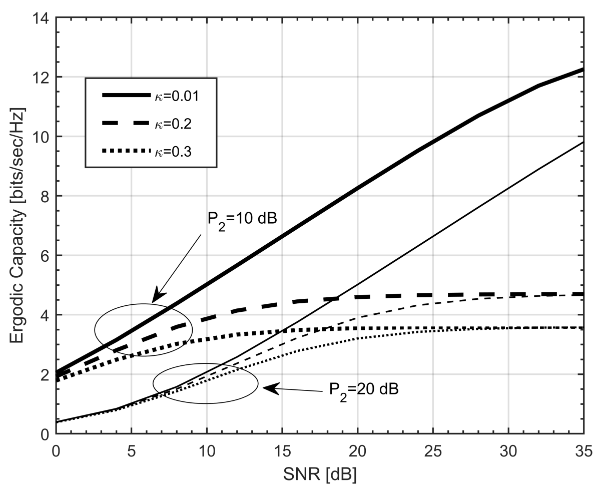

Fig. 5. Ergodic capacity for a hybrid beamforming mmWave network model under RF power leakage constraint and transceiver distortion parameters $\kappa = 0.01; 0.2; 0.3$.

VI. Conclusion

In this paper, we quantified the effects of RF power leakage and hardware transceiver distortion noise on the outage probability and ergodic capacity performance of a mmWave network. A base station uses a hybrid beamforming structure and SDMA to enable multi-user communication with maximum sub-array transmission diversity. Our results indicated that hardware impairment level and RF power leakage significantly affect the OP and ergodic capacity performance. The maximum sub-array transmission diversity technique has considerably improved the system performance, and thus reduces the negative effects of transceiver hardware impairments and RF power leakage in mmWave communication at the cost of requiring the implementation of more sub-arrays.

Appendix A
Proof of Proposition 1

The ergodic capacity is evaluated as follows

$$C = \underbrace{\int_0^\infty \log_2(1+(a+b+c)y) f_Y(y)dy}_{A_1} - \underbrace{\int_0^\infty \log_2(1+(b+c)y) f_Y(y)dy}_{A_2}. \tag{16}$$

We evaluate the A_1 integral by using (8) and a change of variables $\frac{y}{\beta} = z$ and $dy = \beta dz$ leading to

$$A_1 = \frac{1}{\Gamma(mN_s)} \int_0^\infty \log_2(1+(a+b+c)\beta z) z^{mN_s-1} e^{-z} dz. \tag{17}$$

Next, by applying [16, Eq 4.222.8] we solve the integral in (17) as

$$A_1 = \frac{1}{\Gamma(mN_s)\ln(2)} \sum_{i=0}^{mN_s-1} \frac{(mN_s-1)!}{(mN_s-1-i)!} \left(\frac{(-1)^{mN_s-i-2} e^{\frac{1}{(a+b+c)\beta}}}{((a+b+c)\beta)^{mN_s-1-i}} \times Ei(-\frac{1}{(a+b+c)\beta}) + \sum_{k=1}^{mN_s-1-i} \frac{(k-1)!}{(-(a+b+c)\beta)^{mN_s-1-i-k}} \right), \tag{18}$$

where $m-1>0$. Similarly, we calculate A_2 integral in (16) and present the final expression for the ergodic capacity in (13).

Appendix B
Proof of Proposition 2

A lower bound for the ergodic capacity is evaluated by using (14) as

$$C_l^{\mathrm{Nak}} = \log_2\left(1+\exp\left(\underbrace{\int_0^\infty \ln(ay) f_Y(y)dy}_{B_1} - \underbrace{\int_0^\infty \ln((b+c)y+1) f_Y(y)dy}_{B_2}\right)\right). \tag{19}$$

By using [16, Eq. 4.352.1], we evaluate the integral in B_1 as

$$\begin{aligned} B_1 &= \frac{1}{\Gamma(mN_s)\beta^{mN_s}} \int_0^\infty \ln(ay) y^{mN_s-1} e^{\frac{y}{\beta}} dy \\ &= \ln(a) + \psi(mN_s) - \ln(\frac{1}{\beta}) = \ln(a\beta) + \psi(mN_s). \end{aligned} \tag{20}$$

Furthermore, we evaluate B_2 integral by using [16, Eq 4.222.8] as

$$\begin{aligned} B_2 &= \frac{1}{\Gamma(mN_s)\beta^{mN_s}} \int_0^\infty \ln((b+c)y+1) y^{mN_s-1} e^{\frac{y}{\beta}} dy \\ &= \ln(1+(b+c)mN_s\beta). \end{aligned} \tag{21}$$

Finally, by using B_1 and B_2 integral evaluations and (19) we present a lower bound for the ergodic capacity in (15).

References

[1] B. Yang, Z. Yu, J. Lan, R. Zhang, J. Zhou, and W. Hong, "Digital beamforming-based massive MIMO transceiver for 5G millimeter-wave communications," *IEEE Trans. on Microw. Theory and Tech.*, vol. 66, no. 7, pp. 3403–3418, July 2018.

[2] S. Gimenez, S. Roger, P. Baracca, D. Martín-Sacristán, J. F. Monserrat, V. Braun, and H. Halbauer, "Performance evaluation of analog beamforming with hardware impairments for mmW massive MIMO communication in an urban scenario," *Sensors*, vol. 16, no. 10, p. 1555, October 2016.

[3] S. S. Ioushua and Y. C. Eldar, "A family of hybrid analog–digital beamforming methods for massive MIMO systems," *IEEE Trans. on Signal Process.*, vol. 67, no. 12, pp. 3243–3257, June 2019.

[4] K. Satyanarayana, M. El-Hajjar, P. Kuo, A. Mourad, and L. Hanzo, "Dual-function hybrid beamforming and transmit diversity aided millimeter wave architecture," *IEEE Trans. on Veh. Technol.*, vol. 67, no. 3, pp. 2798–2803, March 2018.

[5] D. Zhang, Y. Wang, X. Li, and W. Xiang, "Hybridly connected structure for hybrid beamforming in mmWave massive MIMO systems," *IEEE Transactions on Communications*, vol. 66, no. 2, pp. 662–674, Feb 2018.

[6] A. F. Molisch, V. V. Ratnam, S. Han, Z. Li, S. L. H. Nguyen, L. Li, and K. Haneda, "Hybrid beamforming for massive MIMO: A survey," *IEEE Commun. Magazine*, vol. 55, no. 9, pp. 134–141, Sep. 2017.

[7] Y. Wu, Y. Gu, and Z. Wang, "Channel estimation for mmwave MIMO with transmitter hardware impairments," *IEEE Commun. Lett.*, vol. 22, no. 2, pp. 320–323, Feb 2018.

[8] M. Sadek, A. Tarighat, and A. H. Sayed, "A leakage-based precoding scheme for downlink multi-user MIMO channels," *IEEE Trans. on Wireless Commun.*, vol. 6, no. 5, pp. 1711–1721, May 2007.

[9] K. Venugopal, M. C. Valenti, and R. W. Heath, "Device-to-device millimeter wave communications: Interference, coverage, rate, and finite topologies," *IEEE Trans. on Wireless Commun.*, vol. 15, no. 9, pp. 6175–6188, Sept 2016.

[10] J. G. Andrews, T. Bai, M. N. Kulkarni, A. Alkhateeb, A. K. Gupta, and R. W. Heath, "Modeling and analyzing millimeter wave cellular systems," *IEEE Trans. on Commun.*, vol. 65, no. 1, pp. 403–430, Jan 2017.

[11] S. Kusaladharma, Z. Zhang, and C. Tellambura, "Interference and outage analysis of random D2D networks underlaying millimeter-wave cellular networks," *IEEE Trans. on Commun.*, vol. 67, no. 1, pp. 778–790, Jan 2019.

[12] L. Tlebaldiyeva, B. Maham, and T. A. Tsiftsis, "Device-to-device mmwave communication in the presence of interference and hardware distortion noises," *IEEE Commun. Lett.*, vol. 23, no. 9, pp. 1607–1610, Sep. 2019.

[13] D. Kurita, D. Kitayama, K. Tateishi, A. Harada, Y. Kishiyama, S. Itoh, H. Murai, J. J. Fwu, X. J. Zhuang, K. Stewart, A. Simonsson, and P. Ökvist, "Outdoor experiments on 5G radio access using BS and UE beamforming in 28-GHz frequency band," in *2019 16th IEEE Annual Consumer Commun. Netw. Conf. (CCNC)*, Jan 2019, pp. 1–6.

[14] N. Deng, M. Haenggi, and Y. Sun, "Millimeter-wave device-to-device networks with heterogeneous antenna arrays," *IEEE Trans. on Commun.*, vol. 66, no. 9, pp. 4271–4285, Sep. 2018.

[15] T. Schenk, *RF Imperfections in High-Rate Wireless Systems: Impact and Digital Compenstion*. Springer, 2008.

[16] I. Ryzhik and I. Gradshtein, *Table of integrals, series and products*, 6th ed. San Diego, 2000.